J. Biochem. 129, 365–372 (2001)

Two New Modes of Smooth Muscle Myosin Regulation by the Interaction between the Two Regulatory Light Chains, and by the S2 Domain[1]

Kaoru Konishi,*,† Shin-ichiro Kojima,* Tsuyoshi Katoh,† Michio Yazawa,† Kazuo Kato,* Keigi Fujiwara,* and Hirofumi Onishi*,[2]

Department of Structural Analysis, National Cardiovascular Center Research Institute, Fujishiro-dai, Suita, Osaka 565-8565; and †Division of Chemistry, Graduate School of Science, Hokkaido University, Kita-ku, Sapporo, Hokkaido 060-0810

Received September 27, 2000; accepted December 9, 2000

Previous studies indicated that single-headed smooth muscle myosin and S1 (a single head fragment) are not regulated through phosphorylation of the regulatory light chain (RLC). To investigate the importance of the double-headedness of myosin and of the S2 region for the phosphorylation-dependent regulation, we made three types of recombinant mutant smooth muscle HMMs with one intact head and an N-terminally truncated head. The truncated head of ΔMD lacked the motor domain, that of Δ(MD+ELC) lacked the motor and essential light chain binding domains, and single-headed HMM had one intact head alone. The basal ATPase activities of the three mutants decreased as the KCl concentration became less than 0.1 M. Such a decrease was not observed for S1, which had no S2 region, suggesting that S2 is necessary for this myosin behavior. This activity decrease also disappeared when RLCs of ΔMD and Δ(MD+ELC), but that of single-headed HMM, were phosphorylated. When their RLCs were unphosphorylated, the three mutants exhibited similar actin-activated ATPase levels. However, when they were phosphorylated, the actin-activated ATPase activities of ΔMD and Δ(MD+ELC) increased to the S1 level, while that of single-headed HMM remained unchanged. Even in the phosphorylated state, the actin-activated ATPase activities of the three mutants and S1 were much lower than that of wild-type HMM. We propose that S2 has an inhibitory function that is canceled by an interaction between two phosphorylated RLCs. We also propose that a cooperative interaction between two motor domains is required for a higher level of actin activation.

Key words: interaction between two regulatory light chains, head-S2 interaction, N-terminally truncated HMM, phosphorylation-dependent regulation, smooth muscle myosin.

Phosphorylation of the regulatory light chain (RLC) of myosin is a key reaction for the regulation of smooth muscle contraction. Under unphosphorylated conditions, myosin exhibits low actin-activated ATPase activity (*1–3*) and fails to move actin filaments (*4*). Phosphorylation enhances the ATPase activity by 50–100-fold (*1–3*), and enables myosin to move actin filaments (*4*). Phosphorylation of smooth muscle myosin is known to affect the equilibrium between two different conformational states; an extended 6 S form, in which the tail is extended, and a folded 10 S form, in which the tail is folded into thirds (*5*, *6*). Phosphorylation stabilizes the extended 6 S conformation under physiological conditions, allowing myosin to form thick filaments (*7*, *8*).

The smooth muscle myosin molecule has a double-headed structure with two globular heads connecting to an alpha-helical coiled coil tail. Each head is composed of a motor domain containing an ATPase site and an actin binding site, an essential light chain (ELC) binding domain, and a RLC binding domain. The tail of this molecule is further divided into two domains, the subfragment 2 (S2) domain, which comprises one-third of the tail from the N-terminus, and light meromyosin domain, which comprises the rest of the tail and is responsible for the filament assembly. Previous studies on myosin constructs lacking one or more functionally important domains have provided insights into the way by which phosphorylation could regulate the function of myosin. For example, HMM, which is a soluble double-headed fragment of myosin, is fully regulated by phosphorylation (*9–11*), while the phosphorylation cannot regulate S1, a fragment corresponding to a single head of myosin (*12*). Single-headed myosin lacking one of the two heads,

[1] This work was supported by Research Grants for Cardiovascular Diseases from the Ministry of Health and Welfare of Japan, Grants-in-Aid for Scientific Research from the Ministry of Education, Science and Culture of Japan, and Special Coordination Funds for Promoting Science and Technology from the Science and Technology Agency of Japan (to H.O. and K.F.). S.K. is the recipient of a Domestic Research Fellowship from the Japan Science and Technology Corporation.

[2] To whom correspondence should be addressed: Tel: +81-6-6833-5012, Fax: +81-6-6872-8092, E-mail: honishi@ri.ncvc.go.jp

Abbreviations: ELC, essential light chain; HC, heavy chain; HMM, heavy meromyosin; RLC, regulatory light chain; S1, myosin subfragment 1; S2, myosin subfragment 2.

prepared by proteolytic digestion of smooth muscle myosin, is also poorly regulated by phosphorylation (*13*, *14*). These findings appear to indicate that some interaction between the two heads is necessary for myosin regulation. Analysis of HMMs with differently truncated S2 regions clarified the roles of S2 in phosphorylation-dependent regulation of actin activation. Sata *et al.* have claimed that the upper 1/2–2/3 of the S2 region is required for formation of the double-headed structure of the myosin molecule and for the two heads to interact (*15*). Trybus *et al.* have proposed that the S2 region is actively involved in the regulation of smooth muscle myosin (*16*). Despite their double-headedness, HMMs lacking some part of the S2 region lost the ability of phosphorylation-dependent regulation of the actin-activated ATPase and actin sliding activities. However, it remains unknown whether the head-S2 interaction is critical for the regulation or the S2 region influences the regulation via some modulation of the head–head interaction.

Here, we address this problem by analyzing a series of recombinant HMMs, of which one heavy chain (HC) is truncated (Fig. 1). Previous proteolytic methods could only yield single-headed myosin with one ELC and one RLC, like our single-headed HMM construct. We took advantage of the baculovirus expression system to create two other constructs, ΔMD and Δ(MD+ELC). We here report the results of enzymatic analyses of the three truncated HMMs as well as of recombinant S1 and wild-type HMM. Comparison of their properties lead us to two conclusions. One is that the head-S2 interaction inhibits the myosin function and that this effect is canceled by the interaction between two phosphorylated RLCs. The other is that some intramolecular interaction between two motor domains is necessary for a high level of actin activation.

MATERIALS AND METHODS

Protein Preparation—F-Actin was prepared from rabbit skeletal muscle as described (*17*). Myosin light chain kinase was prepared from chicken gizzard according to Adelstein and Klee (*18*), and calmodulin from bovine testis according to Yazawa *et al.* (*19*).

Construction of Recombinant Baculoviruses—Three types of N-terminally truncated HMM HC constructs [ΔMD, Asp 789–Val 1316; Δ(MD+ELC), Lys 810–Val 1316; and single-headed HMM, Leu 835–Val 1316] were prepared, as follows. GMH-5 (*20*), a cDNA encoding the C-terminal half (Phe 730–Thr 1318) of the chicken gizzard HMM HC, was in vitro mutagenized by the method of Kunkel (*21*). Three different oligonucleotides (the underlined bases indicate the mutations imposed), 5′-TGTGATCTTCAGGTCCATGGCTTCTTCCAGGTGTGC-3′,5′-TCTTGGCAAAGGCCTCCATGGCCAGGTAGCCTCGGCA-3′, and 5′-GCCAGTTCCTCAGCTCCATGGAAGCAGCACAATTTCT-3′, were used to create a *Nco*I site around the Arg 788, Arg 808, and Leu 833 codons, respectively. The mutagenized cDNAs were digested with *Nco*I and *Bst*PI, and the fragments of 0.20 kb (for ΔMD), 0.13 kb (for Δ(MD+ELC), and 0.06 kb (for single-headed HMM) were inserted into the *NcoI*/*Bst*PI site of pFastBacHT-C-HMM-myc (*22*) to obtain transfer vectors for the expression of N-terminal truncated HMM HCs with a N-terminal His-tag. These transfer vectors are named pFastBacHT-ΔMD-myc, pFastBacHT-Δ(MD+ELC)-myc, and pFastBacHT-sh-HMM-myc, respectively.

The transfer vector encoding a full-length HMM HC without a His-tag was produced by removing a His-tag sequence from pFastBacHTa (Life Technologies). Briefly, a *Nco*I site was generated upstream of the His-tag sequence by site-directed mutagenesis (Quick Change Site-Directed Mutagenesis Kit; Stratagene) using two primers; 5′-CGGTCCGAAACCATGGCGTACTACCATCAC-3′, and 5′-GTGATGGTAGTACGCCATGGTTTCGGACCG-3′. The mutagenized pFastBacHTa was digested with *Nco*I to remove a small fragment containing a His-tag sequence, and then the remaining fragment was recircularized (named pFastBacNN). The construction of pFastBacNN-WT-myc, which contains cDNA sequences of the HMM HC (Met 1–Val 1316) plus a C-terminal myc-tag, was performed essentially according to (*22*) except for the use of pFastBac NN, instead of pFastBacHTa.

An S1 HC construct was prepared as follows. To introduce a *Sma*I site at the C-terminus of the S1 HC, GMH-5 was mutagenized by the method of Kunkel (*21*) with an oligonucleotide, 5′-CTGTAGCCCGGGTTTCACTTTGGTGAACAG-3′. A myc-tag coding sequence was synthesized from a pair of oligonucleotides and linked to the C-terminus of the S1 HC by *Sma*I/*Bam*HI site ligation. A cDNA consisting of the HC (Phe 730–Lys 847) and the myc tag was recovered by digestion with *Xba*I (originating from the cloning vector sequence) and *Eco*RI, and inserted into the *Eco*RI/*Xba*I site of pFastBacHTa to obtain pFastBacHT-C-S1-myc. The transfer vector encoding the full-length S1 HC (named pFastBacHT-S1-myc) was obtained by inserting a cDNA fragment encoding the N-terminal half (Met 1–Glu 729) into the *Nco*I/*Eco*RI site of pFastBac-C-S1-myc.

All the recombinant viruses except AcNPV/ELC/RLC (for ELC and RLC) were produced from the above transfer plasmid according to the manufacturer's instructions (Life Technologies). AcNPV/ELC/RLC was prepared as described previously (*23*).

Preparation of Recombinant HMMs and S1—Preparation of His- and myc-tagged wild-type HMMs was carried out as described by Kojima *et al.* (*22*). His- and myc-tagged S1 was prepared by essentially the same method as that used for the tagged wild-type HMM.

Three N-terminally truncated HMMs were prepared as follows. Sf9 cells were coinfected with three viruses; one for both light chains, another for the non His-tagged full-length HMM HC, and the third for a His-tagged N-terminally truncated HMM HC (Asp 789–Val 1316, Lys 810–Val 1316, or Leu 835–Val 1316). The virus-to-cell ratio was 6 for each of the three types of viruses. Three types of proteins (a homodimer of non His-tagged full-length HMM HCs, a homodimer of His-tagged truncated HMM HCs, and a heterodimer of non His-tagged wild-type and His-tagged truncated HMM HCs) were produced in Sf9 cells. The non His-tagged full-length homodimer and His-tagged heterodimer bound to F-actin, and were pelleted by ultracentrifugation (10,000 ×*g*, 20 min). By homogenizing the pellet in 1 mM ATP, both HMMs were dissociated from F-actin. After F-actin had been pelleted by centrifugation at 100,000 ×*g* for 20 min, the supernatnant was incubated at 4°C for 1.5 h with Ni^{2+}-NTA resin (QIAGEN) and then placed in a column. The non His-tagged full-length homodimer was washed out from this column with C-buffer [20 mM Tris-

HCl (pH 7.5), 100 mM KCl, 5 mM 2-mercaptoethanol, and 1 μg/ml leupeptin], and then the C-buffer containing 20 mM imidazole. The His-tagged heterodimer attached to the Ni^{2+}-NTA resin was eluted with the C-buffer containing 100 mM imidazole. Approximately 0.25 mg of the purified proteins was obtained from 1.3 g of Sf9 cells. The molecular masses of the wild-type HMM, ΔMD, Δ(MD+ELC), single-headed HMM, S1, and actin used were 378, 292, 272, 250, 133, and 42 kDa, respectively.

Gel Electrophoresis—SDS-PAGE was carried out according to the method of Laemmli (*24*) usually with a 10% polyacrylamide gel. Native-PAGE was carried out as described (*14*, *25*). The band intensity was determined by densitometry (Personal Densitometer SI, Molecular Dynamics, Sunnyvale, CA, USA).

Electron Microscopy—Electron microscopy was performed with a Hitachi H-800 electron microscope operated at 75 kV. HMM samples were diluted to 10 μg/ml with 70% glycerol and 0.4 M ammonium acetate. These samples were sprayed on to mica and then rotary-shadowed with platinum (*26*, *27*).

ATPase Assay—EDTA (K^+)-ATPase activity measurements were carried out in 0.03 mg/ml HMM or S1, 0.6 M KCl, 10 mM EDTA, 0.2 mM $MgCl_2$, 20 mM Tris-HCl (pH 8.0), 0.2 mg/ml BSA, and 1 mM ATP. The basal Mg^{2+}-ATPase activity was measured as a function of the KCl concentration (from 0.01 to 0.4 M) in an assay medium containing 0.2 mg/ml HMM or S1, 2 mM $MgCl_2$, 20 mM Tris-HCl (pH 7.5), 0.2 mg/ml BSA, 1 mM DTT, 1 mM ATP, and 0.5 mM EGTA or 0.1 mM $CaCl_2$, 4 μg/ml myosin light chain kinase and 1 μg/ml calmodulin. Actin-activated ATPase activity was measured as a function of the F-actin concentration (from 0 to 200 μM) in an assay medium containing 0.05 to 0.15 mg/ml HMM, 20 mM Tris-HCl (pH 7.5), 10 mM KCl, 2 mM $MgCl_2$, 1 mM DTT, 1 mM ATP, and 0.5 mM EGTA or 0.1 mM $CaCl_2$, 4 μg/ml myosin light chain kinase and 1 μg/ml calmodulin. Each reaction was started by adding ATP and stopped by adding perchloric acid to a final concentration of 0.18 M. All assays were preformed at 25°C. The amounts of released inorganic phosphate were determined by the malachite-green method (*28*).

RESULTS

Characterization of N-Terminally Truncated HMMs—In order to prepare three truncated smooth muscle HMMs, ΔMD, Δ(MD+ELC), and single-headed HMM (Fig. 1), three sets of recombinant baculoviruses encoding both light chains, a non–His-tagged full-length HMM HC, and one of the three truncated HMM HC with a His-tag fused at their N-termini were co-infected into Sf9 insect cells. Each polypeptide chain was coexpressed in Sf9 insect cells. Through this coexpression procedure, three types of HMMs, *viz.*, a homodimer of full-length HCs, a heterodimer of full-length and truncated HCs, and a homodimer of truncated HCs, could be formed in the cells. The first and second species formed complexes with actin, and were separated from the third type, which lacked the actin binding site, as pellets by ultracentrifugation. The presence of His-tags at the N-terminis of the truncated HMM HCs allowed us to purify the heterodimers by Ni^{2+}-NTA resin affinity column chromatography. The isolated truncated HMMs, wild-type HMM, and S1 were analyzed by denatured and native gel electrophoreses (Fig. 2). The SDS-PAGE patterns showed that wild-type HMM and S1 each contained a single species of HC, 140 kDa wild-type HC and 94 kDa S1 HC, respectively, and two kinds of light chains in the molar ratio of HC:ELC:RLC = 1:1:1, as determined by densitometry (Fig. 2A). Each of the truncated HMMs, *viz.*, ΔMD, Δ(MD +ELC), or single-headed HMM, contained the wild-type HC and 53 kDa ΔMD HC, 51 kDa Δ(MD +ELC) HC, or 48 kDa single-headed HMM HC, respectively, and also contained both light chains in the molar ratio of wild type HC:ELC:RLC = 1:2:2, 1:1:2, or 1:1:1, respectively. The native-PAGE patterns (Fig. 2B) showed that each of the three different heterodimers moved as a single band. These truncated HMMs were further examined by electron microscopy (Fig. 3). Each truncated HMM showed one globular head and a tail, of which the sizes were similar to those of wild-type HMM. In addition to the regular structure, ΔMD and Δ(MD+ELC) showed small nub-like trun-

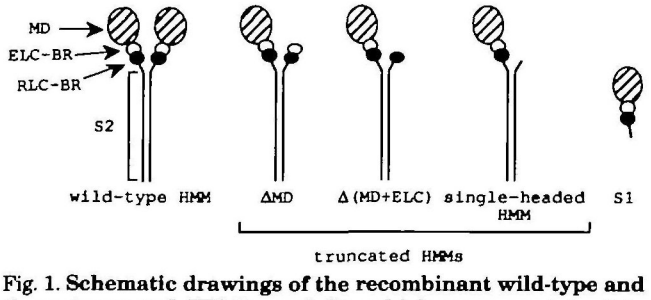

Fig. 1. **Schematic drawings of the recombinant wild-type and three truncated HMMs, and S1, which were used in this study.** Wild-type HMM has two heads, each of which is composed of a motor domain (MD), an ELC binding region (ELC-BR), and a RLC binding region (RLC-BR), and a subfragment 2 region (S2). ΔMD contains only one MD but two ELC and RLC binding regions. Δ (MD+ELC) is a truncated HMM with one MD, and one ELC and two RLC binding regions. Single-headed HMM consists of one each of MD, and ELC and RLC binding regions. While these HMMs have an S2 region, S1 with one each of MD, and ELC and RLC binding regions has no S2 region.

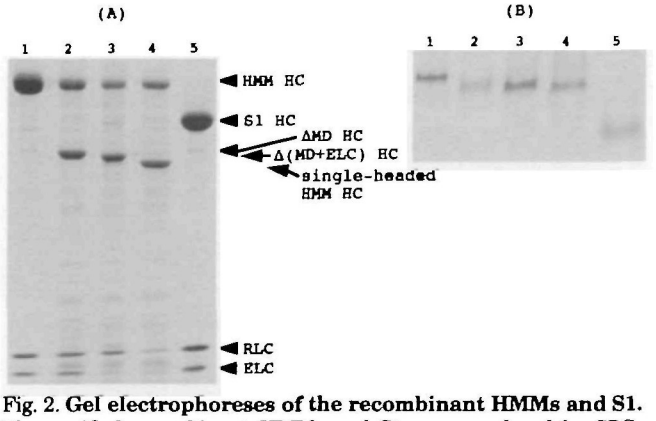

Fig. 2. **Gel electrophoreses of the recombinant HMMs and S1.** The purified recombinant HMMs and S1 were analyzed by SDS-PAGE (A) and native-PAGE (B) . Wild-type HMM (lane 1), ΔMD (lane 2), Δ(MD+ELC) (lane 3), single-headed HMM (lane 4), and S1 (lane 5).

cated heads, the nub of the former appearing larger than that of the latter. The EDTA (K^+)-ATPase activities (per head) of the three truncated HMMs and S1 were essentially the same as that of wild-type HMM (Table I). This suggests that all the recombinant proteins obtained here are homogeneous and correctly folded.

KCl-Concentration Dependency of Basal ATPase Activity—Previous electron microscopy and ultracentrifugation studies revealed that the ATPase activity decrease of HMM is correlated with the conformational transition from the extended 7.5 S to the flexed 9 S conformation (*29*, *30*). When the KCl concentration was lowered from 0.4 to 0.01 M, the basal ATPase activity of unphosphorylated wild-type HMM decreased, and the activity was increased by phosphorylation of RLCs (Fig. 4, panel A). In contrast, the ATPase activity of S1 increased as the KCl concentration was reduced, and the profile of ATPase activity was independent of the phosphorylation state (Fig. 4, panel B). This suggests that S1 can not assume the conformation with low activity corresponding to the 9 S form of HMM.

To assess the ability of the conformational change of the truncated HMMs, their basal ATPase activities were measured at a series of KCl concentrations between 0.4 and 0.01 M (Fig. 4, panels C, D, and E). In the unphosphorylated state, the three truncated HMMs showed similar KCl concentration-dependent decreases in the activity, although a much lower KCl concentration was required. Since these truncated HMMs, but not S1, have the S2 region, it appears that S2 acts as an inhibitory domain and is necessary for the formation of the low-activity-conformational state. On phosphorylation of RLCs, this activity decrease almost completely lost for ΔMD and Δ(MD+ELC) under low-salt conditions (Fig. 4, panels C and D), whereas for single-headed HMM with a single phosphorylated light chain, the activity decrease was retained under low-salt conditions (Fig. 4, panel E). One of the differences between the former two truncated double-headed HMMs and the latter single-headed one is the number of RLCs. ΔMD and Δ(MD+ELC) have two RLCs but single-headed HMM has only one. These results suggest that the presence of two RLCs in a myosin molecule is important for the regulation leading to abolition of the inhibitory effect under low-salt conditions. It is thus possible that some interaction between the two phosphorylated RLCs occurs.

Actin-Activated ATPase Activities of HMM, S1, and Truncated HMMs—To assess the phosphorylation-dependent regulation of the truncated HMMs, we measured the actin-activated ATPase activities of the truncated HMMs as well as recombinant wild-type HMM and S1. We found that the actin-activated ATPase activity of wild-type HMM was greatly enhanced by phosphorylation while that of S1 was not enhanced at all, suggesting that a single myosin head is not sufficient for the regulation by phosphorylation (Fig. 5, panels A and B). These results are consistent with the previous results for HMM and S1, which have been prepared by proteolytic digestion of smooth muscle myosin (*9–12*). We also found that the actin-activated ATPase activities of ΔMD and Δ(MD+ELC) were enhanced by phosphorylation more than 3-fold (Fig. 5, panels C and D), whereas that of single-headed HMM was not (Fig. 5, panels E). This indicates that regulation of actin-activated ATPase also needs two RLCs. To study this more quantitatively, we calculated the maximum activity (V_{max}) and the apparent dissociation constant for actin (K_d) by fitting our data sets to the equation $V = V_{max}/(1 + K_d/[\text{actin}])$. V_{max} of S1 was significantly lower (about 1/6 times) than that of wild-type HMM in the phosphorylated form, whereas S1 had a K_d value of only about 2.5 times that of HMM (Table II). In the unphosphorylated state, the three truncated HMMs had simi-

TABLE I. **EDTA (K^+)-ATPase activity.** EDTA (K^+)-ATPase activity was measured at 25°C in an assay medium containing 0.03 mg/ml HMM or S1, 0.6 M KCl, 10 mM EDTA, 0.2 mM $MgCl_2$, 20 mM Tris-HCl (pH 8.0), 0.2 mg/ml BSA, 1 mM DTT, and 1 mM ATP. Each value is the average of two measurements.

Sample	Activit (s^{-1} $head^{-1}$)
Wild type HMM	1.76
ΔMD	1.68
Δ(MD+ELC)	1.10
Single-headed HMM	1.37
S1	1.34

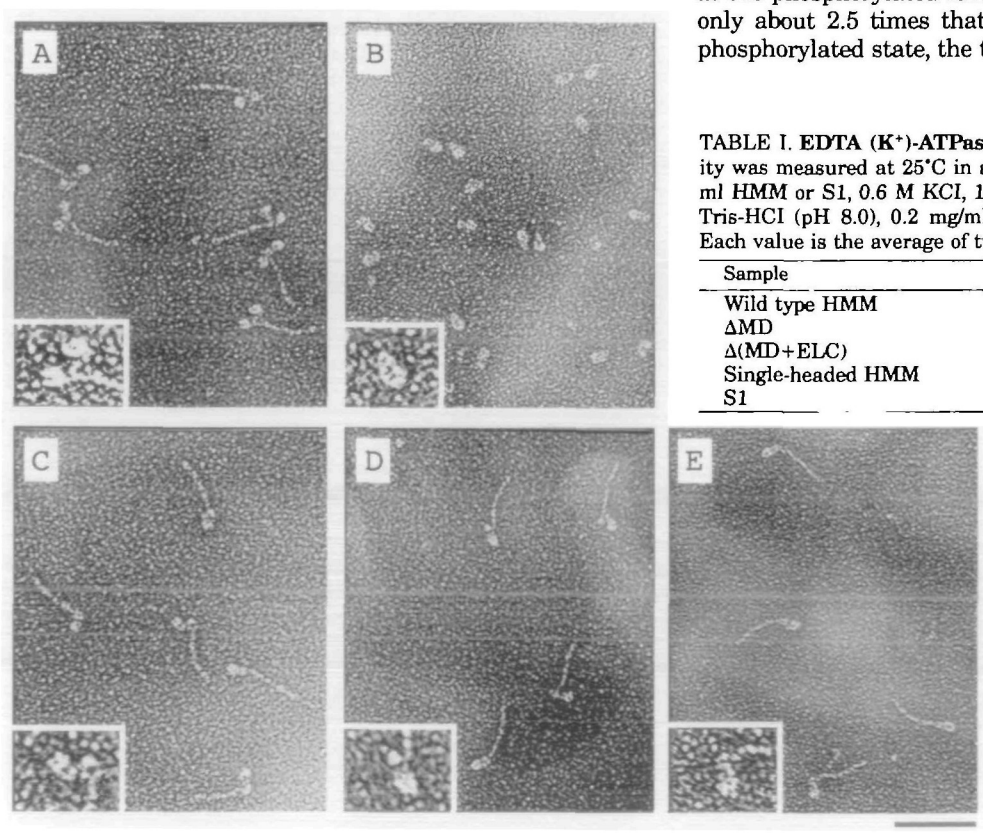

Fig. 3. **Electron microscopy of the recombinant fragments of HMMs and S1.** Metal-shadowed images of wild-type HMM (a), ΔMD (b), Δ(MD+ELC) (c), single-headed HMM (d), and S1 (e). Samples are sprayed on to mica, and then rotary-shadowed with platinum. A two-fold magnified image is shown at the lower left of each panel. Scale bar, 100 nm.

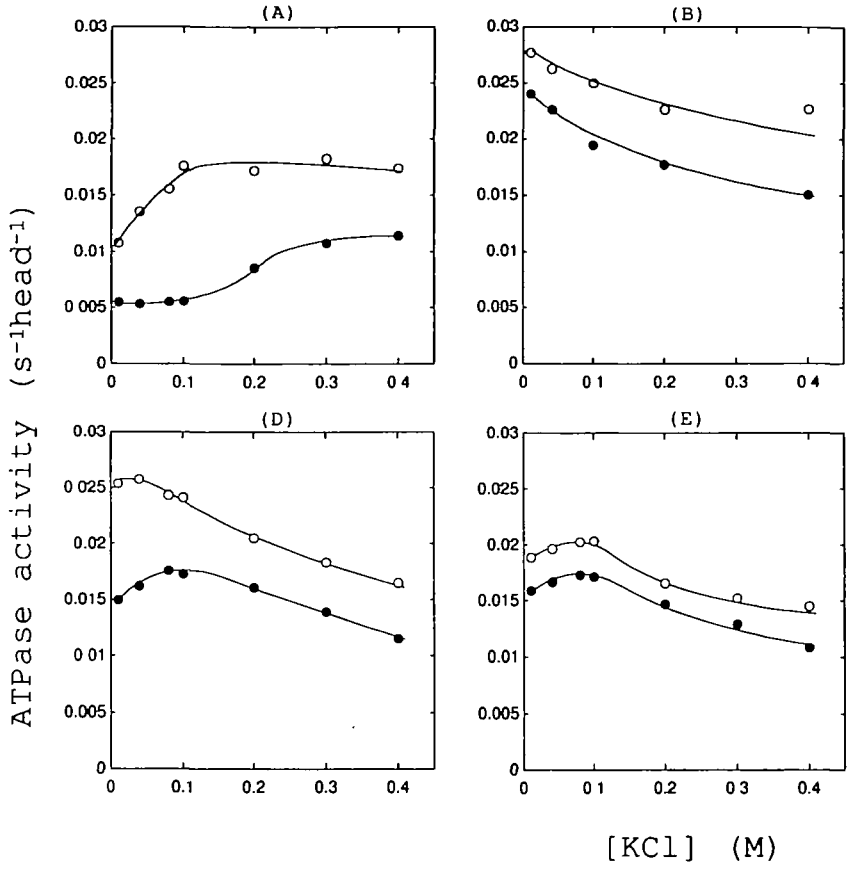

Fig. 4. **Salt concentration–dependence of the basal ATPase activities of the recombinant HMMs and S1.** Mg^{2+}-ATPase activities of wild-type HMM (A), S1 (B), ΔMD (C), Δ(MD +ELC) (D), and single-headed HMM (E) as a function of the KCl concentration. Activities were measured at 25°C with various KCl concentrations, from 0.01 to 0.4 M, in 2 mM $MgCl_2$, 20 mM Tris-HCl (pH 7.5), 0.2 mg/ml BSA, 1 mM DTT, and 1 mM ATP, with 0.5 mM EGTA (● for the unphosphorylated state), or 0.1 mM $CaCl_2$, 4 μg/ml myosin light chain kinase and 1 μg/ml calmodulin (○ for the phosphorylated state). Each assay was started by adding ATP.

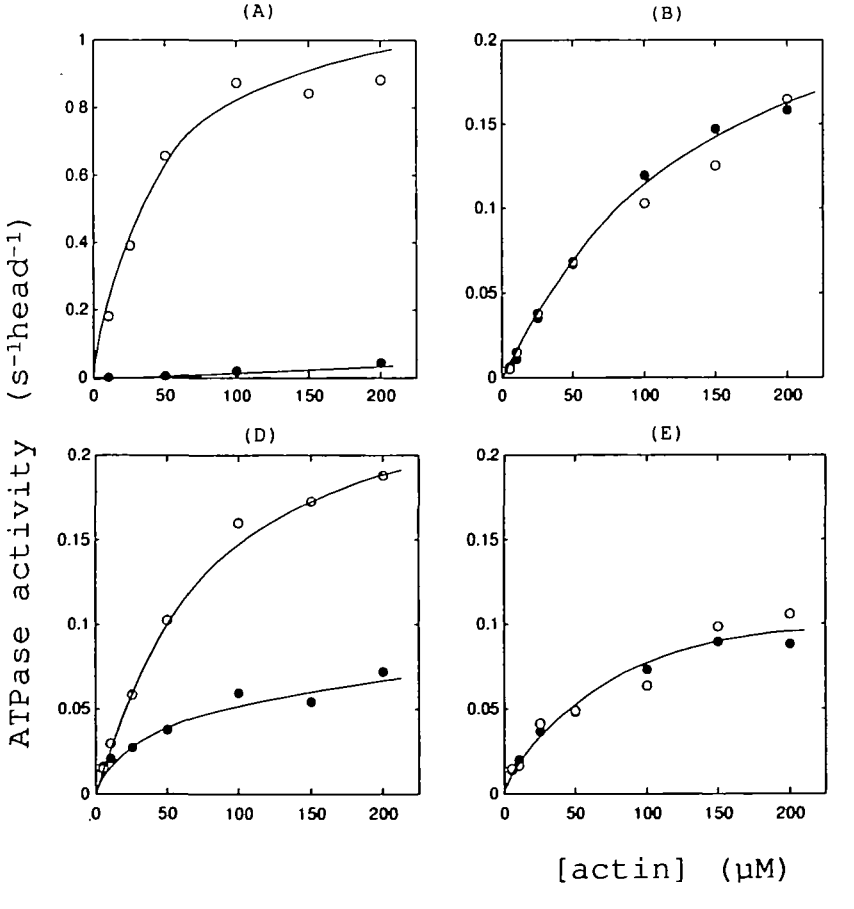

Fig. 5. **Actin-activated ATPase activities of recombinant HMMs and S1.** Actin-activated ATPase activities of wild-type HMM (A), S1 (B), ΔMD (C), Δ(MD+ELC) (D), and single-headed HMM (E) as a function of the actin concentration. Actin-activated ATPase activities were measured at 25°C in a medium containing various concentrations (from 0 to 200 μM) of actin, 10 mM KCl, 2 mM $MgCl_2$, 20 mM Tris-HCl (pH 7.5), 1 mM DTT, and 1 mM ATP, with 0.5 mM EGTA (● for the unphosphorylated state), or 0.1 mM $CaCl_2$, 4 μg/ml myosin light chain kinase, and 1 μg/ml calmodulin (○ for the phosphorylated state). The ATPase activities of HMM alone and actin alone were both subtracted from each measured value to estimate actin-activated ATPase activity.

TABLE II. **V_{max} and K_d values for actin-activated ATPase activities and basal Mg^{2+}-ATPase activities.** V_{max} and K_d were estimated from the date shown in Fig. 4 by fitting to the equation $V = V_{max}/(1+K_d/[actin])$. Basal Mg^{2+}-ATPase activities were measured under the same conditions as those for actin-activated ATPase activities, without actin. Each value is the average of two to five measurements. UP and P are the unphosphorylated and phosphorylated states, respectively.

Sample		V_{max} (S^{-1} head^{-1})	K_d (mM)	Basal Mg^{2+}-ATPase activity (S^{-1} head^{-1})
Wild type HMM	UP	(0.05)[a]	—	0.006
	P	1.37	0.06	0.011
ΔMD	UP	0.07	0.07	0.016
	P	0.24	0.07	0.029
Δ(MD+ELC)	UP	0.09	0.06	0.015
	P	0.28	0.09	0.026
Single-headed HMM	UP	0.12	0.08	0.016
	P	0.11	0.08	0.019
S1	UP	0.26	0.18	0.024
	P	0.24	0.13	0.028

[a]This value is for an actin-activated ATPase activity with 200 μM actin.

lar V_{max} values, which were only 40% of that of S1 (Table II). As described previously, the three truncated HMMs but not S1 have the S2 region. Thus, these results suggest that the S2 region also plays an inhibitory role in the actomyosin ATPase system. The V_{max} values of ΔMD and Δ(MD+ELC) in the phosphorylated state were close to that of S1 and much smaller (about 1/6 times) than that of phosphorylated wild-type HMM (Table II). These results indicate that phosphorylation of the two RLCs cancels the inhibitory effect of the S2 region, although the smaller V_{max} values of S1 and the truncated HMMs can be accounted for by another mechanism (see "DISCUSSION").

DISCUSSION

Smooth muscle HMM has two conformational forms with sedimention coefficients ($s_{20,w}$) of 7.5 and 9 S. When RLC is not phosphorylated, $s_{20,w}$ of the molecule increases from 7.5 to 9 S upon a decrease in the KCl concentration from 0.3 to 0.05 M (*29*, *30*). This increase in $s_{20,w}$ is accompanied by a parallel decrease in the basal Mg^{2+}-ATPase activity (*29*, *30*). Electron microscopy has revealed that the 7.5 S molecule has its heads extended away from the tail, whereas HMM in the 9S form has its heads oriented back toward the tail as a flexed form (*29*). Interestingly the phosphorylation of RLC shifts the salt concentration range for the Mg^{2+}-ATPase activity decrease and the conformational change toward lower concentrations. However, S1, which lacks a two-headed structure and an S2 region, shows no salt concentration-dependent decrease in the activity and no conformational change, as reported previously (*12*, *30*). These observations suggest that the orientation of the heads plays an important role in determining the level of myosin ATPase activity. In the present study, we found that three truncated HMMs with one motor domain show similar activity decreases, although the required concentration of KCl shifts from 0.3 M to less than 0.1 M (Fig. 4). From this result, we assume that these truncated HMMs can exist in both inactive (flexed) and active (extended) forms, like wild-type HMM, depending on the concentration of KCl, and that the decrease in the ATPase activity is also due to the increase in the fraction of the flexed form. Therefore, a head and an S2 region are necessary to form the inactive flexed form, suggesting an inhibitory interaction between the head and S2 region.

The actin-activated ATPase activities of S1 and the three truncated HMMs were roughly proportional to the basal ATPase activities determined with 0.01 M KCl, presumably because no head-head interaction was possible in these molecules. For example, both the basal and actin-activated ATPase activities of single-headed HMM were similar to those of the unphosphorylated (inactive) forms of ΔMD and Δ(MD+ELC), but these activities were about 2.5-fold smaller than those of S1 (Table II, and Figs. 4 and 5). As discussed above, the decrease in the basal ATPase activity is correlated with the increase in the fraction of the flexed form. These findings suggest that the actin-activated ATPase activity is also abolished by the head-S2 interaction, which possibly occurs only in the flexed form. Previously, Trybus *et al.* (*16*, *31*) proposed a model in which the S2 region is necessary to maintain the completely inactive state. Our results support their hypothesis. We can add two new ideas to the model. One is that the interaction between S2 and each myosin head can establish an inactive state, although it remains undetermined which parts (motor domain, ELC, or RLC) of the myosin head are involved in the site of interaction with S2. The other is that the two-headed structure is unnecessary for this process.

We have found that the phosphorylation of two RLCs regulates both the basal and actin-activated ATPase activities even if HMM lacks one motor domain and one ELC binding region (Fig. 5 and Table II). This indicates that an interaction between two phosphorylated RLCs, but not between S2 and one phosphorylated light chain, is important for the regulation. After the present paper had been sent for publication, Li *et al.* (*32*) published a paper reporting that a recombinant HMM with two RLCs but with one motor domain [almost the same as Δ(MD+ELC) in this study] exhibited partial regulation, which is consistent with our present result. However, our finding that single-headed HMM, which has one head and the S2 region, exhibites significantly lower basal and actin-activated ATPase activities, compared with those of S1, provided a new insight into the regulatory mechanism; *i.e.*, the S2 region functions as an inhibitory domain and its inhibitory effect is canceled by the interaction between the two phosphorylated RLCs. We think that the transition from the flexed to the extended form is closely related to this inhibition-releasing mechanism. Maybe what happens is that the RLC phosphorylation cancels the inhibition by weakening the special interaction between the head and the S2 region.

Olney *et al.* (*33*) and we (*14*) have previously shown that the extended to folded conformational transition and the salt concentration-dependent Ca^{2+}-ATPase activity of single-headed myosin are phosphorylation-dependent, although the level of regulation is low compared to that of wild-type myosin. Our present observation that single-headed HMM did not show such a phosphorylation-dependent nature is inconsistent with previous ones by Olney *et al.* and us. When myosin folds its tail, the neck region associates with a specific site of the LMM portion, as shown by electron microscopy (*5*). This interaction should not be occur in the case of single-headed HMM, because this molecule has no LMM portion. The interaction between the neck and LMM portion may be regulated by the RLC phosphorylation in a different way from that between the head

and S2 regions. A possible explanation for the phosphorylation-dependent regulation of single-headed myosin is that the regulation of the interaction between the neck and LMM portion may not require the interaction between two phosphorylated RLCs. Further studies are needed to determine whether this explanation is reasonable or not.

In the phosphorylated state, the actin-activated ATPase activity of double-headed (wild-type) HMM was significantly higher than those of S1 and the truncated HMMs with one motor domain (Fig. 5). On V_{max} and K_d values estimation, we found that the higher actin activation was primarily due to a higher V_{max} value (Table II). Similar results were reported previously, V_{max} for HMM is 4–6 times higher than that for S1 (*9*, *12*). The previous report of Trybus *et al.* (*31*) showed the significantly lower actin-activated ATPase activity of a monomeric construct (termed monomeric 15-heptad S1) in comparison with those of dimeric constructs stabilized with leucine zippers. Our explanation for this finding is that some cooperative work between two motor domains is necessary for full enhancement of the actin activation. We previously revealed that when HMM forms a complex with actin, the two HMM heads can be cross-linked with a zero-length cross-linker, suggesting that the two heads are almost in contact in the rigor complex (*34*). A similar head-head contact might occur when the HMM molecules interact with F-actin in the presence of ATP. In such a case, this contact may be involved in the cooperativity between the two heads proposed in the present study.

Previously, we (*14*) and Cremo *et al.* (*13*) demonstrated that single-headed myosin exhibits high actin-activated ATPase activity, which is one-half that of the phosphorylated form of intact myosin. However, the present study has demonstrated that single-headed HMM, which has no LMM region, is in an inactive state regardless of its phosphorylation state (Fig. 5). The discrepancy between single-headed forms of myosin and HMM in the actin-activated ATPase activity may be explained by assuming that two motor domains from different single-headed myosin molecules can also act cooperatively and thus enhance the actin activation, when these molecules form filaments. We have already suggested that the interaction between two RLCs via a S2 region is essential for the phosphorylation-mediated regulation. However, single-headed myosin has only one RLC. Thus, close contact between two RLCs, like in wild type myosin, can not be expected, and as a result the actin-activated ATPase activity is independent of phosphorylation.

In summary, we have found that two RLCs are necessary for regulating the ATPase activity of the smooth muscle actin-HMM system. The role of phosphorylation is to cancel the inhibitory effect of the S2 region. However, the ATPase activity of truncated HMMs with only one motor domain but with two RLCs is only partially activated by actin. Therefore, two myosin motor domains are essential for complete actin activation.

We wish to thank Mrs. Haruyo Sakamoto for her technical assistance.

REFERENCES

1. Small, J.V. and Sobieszek, A. (1990) The contractile apparatus of smooth muscle. *Int. Rev. Cytol.* **64**, 241–306
2. Adelstein, R.S. and Eisenberg, E. (1980) Regulation and kinetics of the actin-myosin-ATP interaction. *Annu. Rev. Biochem.* **49**, 921–956
3. Hartshorne, D.J. and Siemenkowski, R.F. (1981) Regulation of smooth muscle actomyosin. *Annu. Rev. Physiol.* **43**, 519–530
4. Sellers, J.R. (1991) Regulation of cytoplasmic and smooth muscle myosin. *Curr. Opin. Cell Biol.* **3**, 98–104
5. Onishi, H. and Wakabayashi, T. (1982) Electron microscopic studies of myosin molecules from chicken gizzard muscle I: the formation of the intramolecular loop in the myosin tail. *J. Biochem.* **92**, 871–879
6. Trybus, K.M., Huiatt, T.W., and Lowey, S. (1982) A bent monomeric conformation of myosin from smooth muscle. *Proc. Natl. Acad. Sci. USA* **79**, 6151–6155
7. Suzuki, H., Onishi, H., Takahashi, K., and Watanabe, S. (1978) Structure and function of chicken gizzard myosin. *J. Biochem.* **84**, 1529–1542
8. Trybus, K.M. (1991) Assembly of cytoplasmic and smooth muscle myosins. *Curr. Opin. Cell Biol.* **3**, 105–111
9. Onishi, H. and Watanabe, S. (1979) Chicken gizzard heavy meromyosin that retains the two light-chain components, including a phosphorylatable one. *J. Biochem.* **85**, 457–472
10. Seidel, J.C. (1980) Fragmentation of gizzard myosin by alpha-chymotrypsin and papain, the effects on ATPase activity, and the interaction with actin. *J. Biol. Chem.* **255**, 4355–4361
11. Sellers, J.R., Pato, M.D., and Adelstein, R.S. (1981) Reversible phosphorylation of smooth muscle myosin, heavy meromyosin, and platelet myosin. *J. Biol. Chem.* **256**, 13137–13142
12. Ikebe, M. and Hartshorne, D.J. (1985) Proteolysis of smooth muscle myosin by Staphylococcus aureus protease: preparation of heavy meromyosin and subfragment 1 with intact 20,000-dalton light chains. *Biochemistry* **24**, 2380–2387
13. Cremo, C.R., Sellers, J.R., and Facemyer, K.C. (1995) Two heads are required for phosphorylation-dependent regulation of smooth muscle myosin. *J. Biol. Chem.* **270**, 2171–2175
14. Konishi, K., Katoh, T., Morita, F., and Yazawa, M. (1998) Conformation, filament assembly, and activity of single-headed smooth muscle myosin. *J. Biochem.* **124**, 163–170
15. Sata, M., Matsuura, M., and Ikebe, M. (1996) Characterization of the motor and enzymatic properties of smooth muscle long S1 and short HMM: role of the two-headed structure on the activity and regulation of the myosin motor. *Biochemistry* **35**, 11113–11118
16. Trybus, K.M. (1994) Regulation of expressed truncated smooth muscle myosins. Role of the essential light chain and tail length. *J. Biol. Chem.* **269**, 20819–20822
17. Spudich, J.A. and Watt, S. (1971) The regulation of rabbit skeletal muscle contraction. I. Biochemical studies of the interaction of the tropomyosin-troponin complex with actin and the proteolytic fragments of myosin. *J. Biol. Chem.* **246**, 4866–4871
18. Adelstein, R.S. and Klee, C.B. (1981) Purification and characterization of smooth muscle myosin light chain kinase. *J. Biol. Chem.* **256**, 7501–7509
19. Yazawa, M., Sakuma, M., and Yagi, K. (1980) Calmodulins from muscles of marine invertebrates, scallop and sea anemone. *J. Biochem.* **87**, 1313–1320
20. Yanagisawa, M., Hamada, Y., Katsuragawa, Y., Imamura, M., Mikawa, T., and Masaki, T. (1987) Complete primary structure of vertebrate smooth muscle myosin heavy chain deduced from its complementary DNA sequence. Implications on topography and function of myosin. *J. Mol. Biol.* **198**, 143–157
21. Kunkel, T.A. (1985) Rapid and efficient site-specific mutagenesis without phenotypic selection. *Proc. Natl. Acad. Sci. USA* **82**, 488–492
22. Kojima, S., Fujiwara, K., and Onishi, H. (1999) SH1 (cysteine 717) of smooth muscle myosin: its role in motor function. *Biochemistry* **38**, 11670–11676
23. Onishi, H., Maéda, K., Maéda, Y., Inoue, A., and Fujiwara, K. (1995) Functional chicken gizzard heavy meromyosin expression in and purification from baculovirus-infected insect cells. *Proc. Natl. Acad. Sci. USA* **92**, 704–708
24. Laemmli, U.K. (1970) Cleavage of structural proteins during

the assembly of the head of bacteriophage T4. *Nature* **227**, 680–685
25. Trybus, K.M. and Lowey, S. (1985) Mechanism of smooth muscle myosin phosphorylation. *J. Biol. Chem.* **260**, 15988–15995
26. Tyler, J.M. and Branton, D. (1980) Rotary shadowing of extended molecules dried from glycerol. *J. Ultrastruct. Res.* **71**, 95–102
27. Katoh, T. and Morita, F. (1996) Roles of light chains in the activity and conformation of smooth muscle myosin. *J. Biol. Chem.* **271**, 9992–9996
28. Kodama, T., Fukui, K., and Kometani, K. (1986) The initial phosphate burst in ATP hydrolysis by myosin and subfragment-1 as studied by a modified malachite green method for determination of inorganic phosphate. *J. Biochem.* **99**, 1465-1472
29. Suzuki, H., Kamata, T., Onishi, H., and Watanabe, S. (1982) Adenosine triphosphate-induced reversible change in the conformation of chicken gizzard myosin and heavy meromyosin. *J. Biochem.* **91**, 1699–1705
30. Suzuki, H., Stafford, W.F., Slayter, H.S., and Seidel, J.C. (1985) A conformational transition in gizzard heavy meromyosin involving the head-tail junction, resulting in changes in sedimentation coefficient, ATPase activity, and orientation of heads. *J. Biol. Chem.* **260**, 14810–14817
31. Trybus, K.M., Freyzon, Y., Faust, L.Z., and Sweeney, H.L. (1997) Spare the rod, spoil the regulation: necessity for a myosin rod. *Proc. Natl. Acd. Sci. USA* **94**, 48–52
32. Li. X.-d., Saito, J., Ikebe, R., Mabuchi, K., and Ikebe, M. (2000) The interaction between the regulatory light chain domains on two heads is critical for regulation of smooth muscle myosin. *Biochemistry* **39**, 2254–2260
33. Olney, J.J., Sellers, J.R., and Cremo, C.R. (1996) Structure and function of the 10 S conformation of smooth muscle myosin. *J. Biol. Chem.* **271**, 20375–20384
34. Onishi, H., Maita, T., Matsuda, G., and Fujiwara, K. (1990) Lys-65 and Glu-168 are the residues for carbodiimide-catalyzed cross-linking between the two heads of rigor smooth muscle heavy meromyosin. *J. Biol. Chem.* **265**, 19362–19368